

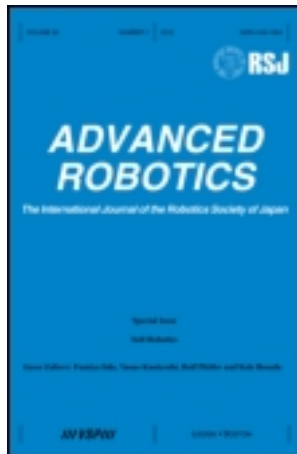
This article was downloaded by: [UQ Library]

On: 16 September 2013, At: 07:57

Publisher: Taylor & Francis

Informa Ltd Registered in England and Wales Registered Number: 1072954

Registered office: Mortimer House, 37-41 Mortimer Street, London W1T 3JH, UK



Advanced Robotics

Publication details, including instructions for authors and subscription information:

<http://www.tandfonline.com/loi/tadr20>

The standard circular gait of a quadruped walking vehicle

Shigeo Hirose ^a, Hidekazu Kikuchi ^b & Yoji Umetani ^c

^a Department of Physical Engineering, Tokyo Institute of Technology, 2-12-1, Ookayama, Myuro-ku, Tokyo 152, Japan

^b Department of Physical Engineering, Tokyo Institute of Technology, 2-12-1, Ookayama, Myuro-ku, Tokyo 152, Japan

^c Department of Physical Engineering, Tokyo Institute of Technology, 2-12-1, Ookayama, Myuro-ku, Tokyo 152, Japan

Published online: 02 Apr 2012.

To cite this article: Shigeo Hirose , Hidekazu Kikuchi & Yoji Umetani (1986) The standard circular gait of a quadruped walking vehicle, Advanced Robotics, 1:2, 143-164, DOI:

[10.1163/156855386X00058](https://doi.org/10.1163/156855386X00058)

To link to this article: <http://dx.doi.org/10.1163/156855386X00058>

PLEASE SCROLL DOWN FOR ARTICLE

Taylor & Francis makes every effort to ensure the accuracy of all the information (the "Content") contained in the publications on our platform. However, Taylor & Francis, our agents, and our licensors make no representations or warranties whatsoever as to the accuracy, completeness, or suitability for any purpose of the Content. Any opinions and views expressed in this publication are the opinions and views of the authors, and are not the views of or endorsed by Taylor & Francis. The accuracy of the Content should not be relied upon and should be independently verified with primary sources of information. Taylor and Francis shall not be liable for any losses, actions, claims, proceedings, demands, costs, expenses, damages, and other liabilities whatsoever or howsoever caused arising directly or indirectly in connection with, in relation to or arising out of the use of the Content.

This article may be used for research, teaching, and private study purposes. Any substantial or systematic reproduction, redistribution, reselling, loan, sub-

licensing, systematic supply, or distribution in any form to anyone is expressly forbidden. Terms & Conditions of access and use can be found at [http://
www.tandfonline.com/page/terms-and-conditions](http://www.tandfonline.com/page/terms-and-conditions)

The standard circular gait of a quadruped walking vehicle

SHIGEO HIROSE, HIDEKAZU KIKUCHI and YOJI UMETANI

*Department of Physical Engineering, Tokyo Institute of Technology, 2-12-1, Ookayama,
Myuro-ku, Tokyo 152, Japan*

Received for JRSJ 3 August 1984; English version received 7 June 1986

Abstract—A quadruped walking vehicle has the potential capability of being developed into a vehicle of high mobility and adaptability to terrain by making use of its high degree of motion freedom. The authors have investigated the gait control problems of a walking vehicle, i.e. the straightforward or crab walk of the vehicle on rough terrains. This paper introduces a more generalized gait, namely, a circular gait around an arbitrarily located turn center, and discusses a standard circular gait. The standard circular gait is the one which maximizes the speed of walking and the rotational angle in a circular walk, and this consideration forms the basis of the discussion on advanced gait control problems. This paper formalizes the problems and analyses them by using mathematical optimization methods such as non-linear programming. Computations are carried out on a TITAN III, the quadruped walking vehicle model constructed by the authors. Several characteristics of the optimum gait and the final gait selection chart are derived. The validity of these conditions was verified by a circular walking experiment using the TITAN III.

1. INTRODUCTION

The current study relates to a gait-determining problem of a quadruped walking vehicle having three degrees of freedom in each leg. We believe it is important to concentrate on the development of a quadruped walking vehicle because (1) the capability of static, stable walking allows diverse technical applications, (2) the load-carrying capacity can be maximized with the simplest mechanism of static walking, (3) the effective use of 12 degrees of freedom can realize highly adaptable mobility, which is impossible with conventional wheeled-vehicles, and (4) the robot performance can be stepped up in the future to that of a high-speed dynamic walking system.

Among the merits stated above, in order to exploit fully the high potential mobility to be provided by a quadruped walking vehicle as pointed out in (3), it is essential to elucidate how a diverse and an efficient gait is to be produced with a four-legged robot. In this connection, we have discussed “straight-forward walking” as the fundamentals of a quadruped walking machine [1], and subsequently defined “crab walking” as a more generalized gait in which the direction of motion makes a random angle with the torso direction of the walking vehicle, and studied standard gait as well as adaptive gait determinations to rough terrains [2].

In addition, a four-legged walking robot with 12 degrees of freedom has the potential capability of motion flexibility. Therefore, it is necessary to study a more generalized gait in order to realize an adaptive and smooth walking function which is possible by fully utilizing the capability of a quadruped walking vehicle.

In our discussion, we concentrate on the subject of ‘turning gait’, which is defined to be the steady circular walking movement, as illustrated in Fig. 2, of the centre of

the torso gravity around a random turning centre Q. One of the cases specified is that the turning centre Q is on the y-axis (the ordinate) in a circular movement, for instance, as observed when a car's steering wheel is turned. As the circling centre is a random point in the XY plane, the torso direction keeps some constant angle with the direction of motion at any moment of the circling movement (this angle corresponds to the lateral moving angle of crab walking, called the lateral circular angle a_Q). When the circling centre is located close to the x-axis (the abscissa), that is, when the lateral circular angle a_Q is close to 90°, the robot performs a crab-like walk towards the y-axis. When the centre is near the origin, the robot performs a rotational walk on the spot, while a centre located at infinite distance makes the circular walking the same as crab walking. In other words, the circular gait of a four-legged robot implies a more generalized walking mode including the gait presented so far.

In designing a gait control system, we have been aiming to select a standard gait which optimizes the walking efficiency, as long as the gait is not affected by the conditions of the terrain.

If the same standpoint is adopted for the control system of circular motion, the 'standard circular gait' and its method of derivation should be clarified for the first time.

A suitable sequence of leg-swing of the standard circular gait is different depending on the position of the turning centre, and the method of determining details of the gait is estimated to be quite different from the conventional approach based on straightforward motion.

In this respect, the current study will (1) clarify various conditions for discussing the standard circular gait and exhibit the optimum conditions A and B required for determining the standard circular gait, (2) obtain the subset of the gait satisfying the optimum condition A, (3) define two representative types of basic leg-swing pattern, based on the maximum number of six combinations of leg-swing pattern possible to make static and stable walking, (4) obtain a gait satisfying the above-stated optimum conditions A and B for respective leg-swing patterns, and (5) obtain the standard circular gait for circular walking around a random turning centre. The paper deals with these points in the order stated above.

2. DEFINITION OF THE PROBLEMS

2.1. Main codes

- a_Q circular crab walk angle
- ϕ_x argument of the polar coordinate expression (γ_x, ϕ_x) of the point X when the origin is set at the circulating centre Q
- θ_i circular angle of the gravity centre during the returning movement of leg i ($i=1$ to 4)
- $\bar{\theta}_i$ circular angle of the gravity centre while leg i is in the supporting phase
- θ circular angle of the gravity centre during a walk of one cycle
- θ'_i ($=\theta_i/\theta$)
- r_i path radius of foot tip of leg i
- r_G path radius of the torso gravity centre G
- r'_i ($=r_i/r_G$)
- V maximum peripheral speed of a leg on the gravity centre coordinate system
- v_i returning peripheral speed of leg i on the gravity centre coordinate system

- V_G maximum circular peripheral speed of the gravity centre against the ground coordinate
- v_{Gi} circular peripheral speed of the gravity centre against the ground when leg i returns
- C_i diagram centre of reachable area of leg i , denoted as (X_{Ci}, Y_{Ci})
- Q circular centre, denoted as (X_q, Y_q)
- G torso gravity centre, denoted as (X_G, Y_G) or (r_G, ϕ_G)
- F_i forehand point of two points at which the arc orbit of leg i crosses its reachable area, denoted as (X_{Fi}, Y_{Fi})
- R_i rearhand point of two points at which the arc orbit of leg i crosses the reachable area, denoted as (X_{Ri}, Y_{Ri})
- P_i position when leg i is at the switching point

2.2. Model of the walking vehicle

The model of the walking vehicle is assumed to be like the one shown in Fig. 1, having four legs, each with a rectangular prism of reachable space. The dimensions of the reachable space are designed to be nearly the same as those of TITAN III [3], the prototype shown in Fig. 13. The test result of the actual circular walk using this machine model is stated in Section 8.2. In addition, the most basic complete flat surface is assumed for the walking environment.

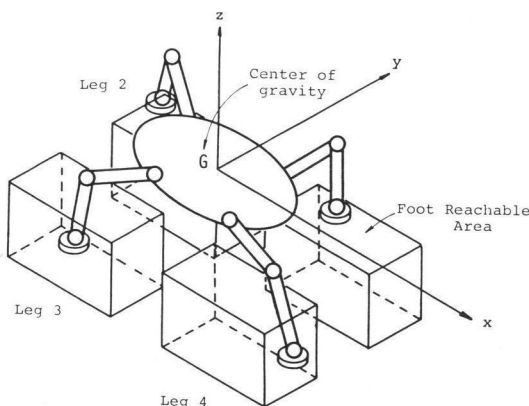


Figure 1. The walking vehicle model.

2.3. Basic conditions related with the walk

The following conditions are set for the performance of the walking vehicle and the basic walking function:

- (1) During the walk, it is assumed that the torso gravity centre is held at constant height and that the foot tips make only two-dimensional movement on the xy plane. In the actual walk, the foot tips should be lifted slightly in the returning movement, even on a flat plane. In other words, z -directional motion is

essentially included at the beginning and end of a returning phase. Nevertheless, for the purpose of simplification, the current study will ignore these z -directional motions and will assume that the foot tips make returning motions which skim the surface of the ground. The speed of the tip motion is assumed to be constant from the beginning to the end of the movement.

- (2) It is assumed that the foot tips cannot move faster than the mechanical maximum swing speed V in any direction in the xy plane. Strictly speaking, a driving mechanism based on xy -directional independent actuators can generate a maximum speed of $\sqrt{(v_x^2 + v_y^2)}$ (where v_x and v_y are the respective maximum speeds), whereas this study assumes the maximum speed to be $V = \min(v_x, v_y)$ for simplicity.
- (3) The walk is assumed to be statistically stable of the duty factor $\beta = 0.75$. The duty factor β is the ratio of the time when a leg is in the supporting phase to the time of a walk of one cycle [4]. When $\beta = 0.75 (= 3/4)$ and the vehicle makes a statically stable walk, the torso is always supported by three legs out of four during a walk, and two- or four-leg support does not take place. At the same time, during this mode the stability allowance might possibly become nil when the free legs switch. This type of gait was defined by Tomović as creep gait [5], which is the most basic one for the consideration of a statically stable walk.

2.4. Conditions specific to circular gait

The following three conditions are specific to the study of circular gait:

- (4) The foot-tip path of leg i in the supporting phase is assumed to pass always through the diagram centre C_i in the rectangular reachable range on the xy plane. In the actual movement, the tip can pass anywhere within the reachable range; however, the above assumption is for simplicity. Our preliminary simulation indicates such a simplification is not detrimental to the obtention of an optimum answer. In previous studies of crab gait, we assumed a standard system in which the foot tip passed through the diagram centre C_i , so that the present condition is reasonable even for combined controls, to be studied hereafter.
- (5) The circular peripheral speed of the gravity centre of the walking vehicle is assumed to be constant.
- (6) The returning motion of the foot tip seen from the gravity centre coordinate system is assumed to move in the inverse direction on the same arc path in the supporting phase at a constant peripheral speed v_r ($i = 1$ to 4). In the returning motion, the foot tips can move independently of the other legs and quick circular motion is also possible by the return of the swing leg in the linear path. Nevertheless, the advantage of increasing the speed of the linear swing is not so great as to justify the complicity of the analysis.

2.5. Conditions of standard circular gait

The standard circular gait will be defined as the gait with the highest walking efficiency satisfying the following two optimum conditions, among all the possible gaits:

Optimum condition A: The condition at which the rotational speed of the gravity centre of the vehicle becomes maximum V_G .

Optimum condition B: The condition which maximizes the travelling angle of the gravity centre θ during a one-cycle walk.

Optimum condition A is given only by the relative ratio of θ_i , regardless of the order of swing legs or the absolute value of θ_i ($i=1$ to 4), the travelling angle of the gravity centre during the returning movement of all four legs. It is because of condition (1) of Section 2.3, by which the rotational speeds do not differ significantly, that the vehicle might walk in a small-swing multi-cycle or in a large-swing small-cycle during its unit angle turn.

Optimum condition B maximizes the travelling angle of the gravity centre θ as much as possible under the restriction of three conditions, i.e. optimum condition A, the condition in which all the legs work in their reachable range, and the condition to implement the order of leg-returns as designed. The walk with a maximum travelling angle is thought to be indispensable, because later when condition (1) of Section 2.3 is removed and the up/down moving time of legs is taken into consideration, it is the best gait for optimizing the energy efficiency and speed of locomotion, taking into account the conceivable energy loss and time loss at acceleration/deceleration of legs.

3. INDUCING PROCEDURE FOR STANDARD CIRCULAR GAIT

In general, determination of the gait of quadruped walking vehicle which moves in a creeping manner requires three procedures: (1) selection of order of leg-returns, (2) selection of shifting amount of gravity centre on the return of each leg, and (3) selection of new landing positions of the returned legs. The induction of the optimized standard circular gait in this paper is to carry out the three procedures in the following steps:

- (1) As the preliminary calculation, the foot-tip path radius r_i of each leg, the circular radius of gravity centre r_G and the argument indicating the reachable range limits ϕ_{F_i} and ϕ_{R_i} as shown in Fig. 2 are induced based on the reachable range of each leg against the turn centre Q, diagram centre C, of each reachable range and the relative positioning of torso gravity centre G.
- (2) Circular angle θ_i of the gravity centre on leg-return, which satisfies optimum condition A, is induced in the form of its ratio θ_i against the circular angle θ at one-cycle walk.
- (3) Candidates of the X, Y and O types of conceivable leg-return orders for the walking vehicle are set.
- (4) Argument ϕ_i of the initial point of foot-landing in the standard gait satisfying both optimum conditions A and B is determined. θ_i is also determined under the conditions that designed free leg order is observed and reachable range of leg i is in $\phi_{R_i} - \phi_{F_i}$.
- (5) A ‘status chart’ [Fig. 11(d)], which determines the order of leg-return maximizing the turning angle θ of the gravity centre, is obtained for all the circular gaits in which the turn centre Q is at a random point in the xy plane.

Thus, when a random turn centre Q is given, it is possible to set all the orders of leg-return ϕ_i , θ_i required for determining the standard circuit gait. Detailed processes will be given in the following sections.

4. PRELIMINARY CALCULATION FOR INDUCTION

Given below are the parameters which should be calculated first when considering the standard patterns:

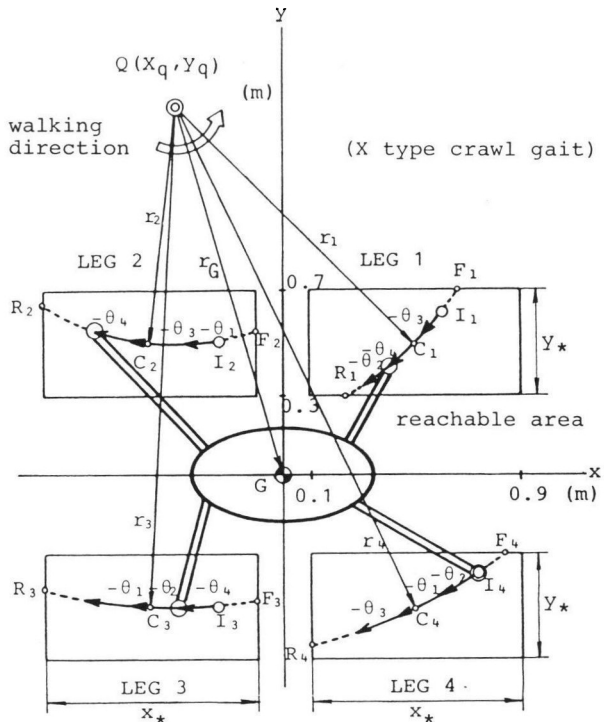


Figure 2. Foot trajectories, model dimensions and parameters of standard circular gait.

- (1) radius of foot-tip path r_i and circular radius of gravity centre r_G to be used for inducing both optimum conditions A and B;
- (2) arguments ϕ_{F_i} and ϕ_{R_i} , which indicate the reachable range limits to be used for inducing optimum condition B.

These can be obtained by a rather simple geometrical calculation: When the turn centre is $Q(X_q, Y_q)$ and the diagram centre of reachable range prisms is $C_i(X_{ci}, Y_{ci})$,

$$\begin{aligned} r_i &= \sqrt{(X_{ci} - X_q)^2 + (Y_{ci} - Y_q)^2} \quad (i=1 \text{ to } 4) \\ r_G &= \sqrt{X_q^2 + Y_q^2}^{1/2}. \end{aligned} \quad (1)$$

Equation (2) can be obtained from the intersection of the arc passing through the diagram centre C_i with rectangular reachable range. That is,

$$(x - X_q)^2 + (y - Y_q)^2 = r_i^2 \quad (2)$$

and

$$\left. \begin{aligned} x &= X_{ci} \pm x_* / 2 & (Y_{ci} - y_*/2 \leq y \leq Y_{ci} + y_*/2) \\ y &= Y_{ci} \pm y_* / 2 & (X_{ci} - x_*/2 \leq x \leq X_{ci} + x_*/2) \end{aligned} \right\}. \quad (3)$$

Of the intersections with either of the above, the one on the forehand position in the direction of motion is F_i and the other on the rearhand is R_i ; the equations are:

$$\left. \begin{aligned} \phi_{F_i} &= \tan^{-1} \frac{Y_{Fi} - Y_q}{X_{Fi} - X_q} \\ \phi_{R_i} &= \tan^{-1} \frac{Y_{Ri} - Y_q}{X_{Ri} - X_q} \end{aligned} \right\} \quad (i=1 \text{ to } 4). \quad (4)$$

By the way, the intersections F_i and R_i do exist when the foot tip is located near the turn centre Q and the small circular path is within the reachable range. In this case, the equations are assumed to be

$$\begin{aligned}\phi_{R_i} &= \phi_{C_i} - \pi, \quad \phi_F \\ i &= \phi_{C_i} + \pi.\end{aligned}\quad (5)$$

5. GAIT REALIZING OPTIMUM CONDITION A

The gait realizing optimum condition A is induced in the following way: First we consider the time t_i required for leg i to complete return motion during a circular walk. If it is assumed that the gravity centre turns by θ_i in this time, and the circular peripheral speed of the gravity centre is v_{Gi} , the equation is

$$t_i = r_G \theta_i / v_{Gi}$$

On the other hand, when the return angle of leg i is considered in the coordinates of the gravity centre within time t_i , the return angle should be equal to the angle when leg i is in the supporting phase, in order to realize a constant cyclic gait. The angle is the total θ_i , the sum of the return angles of the three legs other than leg i , and the relation is $\theta = \theta - \theta_i$, that is, $t_i = r_i(\theta - \theta_i) / v_i$. The following equation is obtained:

$$\frac{r_G \theta_i}{v_{Gi}} = \frac{r_i(\theta - \theta_i)}{V_i} \quad (i=1 \text{ to } 4). \quad (6)$$

Provided that the ratio of the returning peripheral speed v_i of the returning leg i against the gravity centre G with the circular peripheral speed of gravity centre v_{Gi} against the turning axis of the gravity centre is defined as χ_i :

$$\chi_i \equiv \frac{v_i}{v_{Gi}} = \frac{r_i(\theta - \theta_i)}{r_G \theta_i} = r'_i \left(\frac{1}{\theta'_i} - 1 \right) \quad (7)$$

where

$$r'_i \equiv \frac{r_i}{r_G}, \quad \theta'_i \equiv \frac{\theta_i}{\theta} \quad (i=1 \text{ to } 4).$$

According to condition (2) of Section 2.3, $v_i \leq V$, therefore

$$v_{Gi} = \frac{v_i}{\chi_i} \leq \frac{V}{\chi_i} \quad (i=1 \text{ to } 4). \quad (8)$$

However, the maximum circular peripheral speed V_G of the gravity centre is obtained from

$$V_G = \min_{i=1-4} v_{Gi}$$

based on condition (5) denoting the constancy of the circular peripheral speed of the gravity centre. Accordingly,

$$V_G = \frac{V}{\chi_{\max}}, \quad \chi_{\max} \equiv \max_{i=1-4} \chi_i. \quad (9)$$

For V_G to be a maximum under the above-mentioned conditions, all the χ_i are proven to be the same (Appendix A). Therefore,

$$\chi_i = \chi_0 = \text{constant} \quad (i=1 \text{ to } 4). \quad (10)$$

Substituting equation (10) into equation (7) and rearrangement give

$$\theta'_i = \frac{r'_i}{r'_i + \chi_0} \quad (i=1 \text{ to } 4). \quad (11)$$

Here χ_0 is the positive root of the following equation based on the relation

$$\begin{aligned} \sum_{i=1}^4 \theta_i &= \theta: \\ \sum_{i=1}^4 \frac{r'_i}{r'_i + \chi_0} &= \sum_{i=1}^4 \theta'_i = 1. \end{aligned} \quad (12)$$

In other words, the maximum circular speed of the gravity centre $V_G (= V/\chi_0)$ can be obtained by using the value of χ_0 of equation (12), and the return circular angle of each leg can be obtained from equation (11) in the form of distribution rate θ'_i . As a specific case, taking the case of the crab walk gait $r_G \rightarrow \infty$, for example, $r_i \rightarrow \infty$ leads to $r'_i (= r/r_G) \rightarrow 1$ and equation (12) becomes

$$\sum_{i=1}^4 \frac{1}{1 + \chi_0} = \frac{4}{1 + \chi_0} = 1 \quad (13)$$

$$\therefore \chi_0 \left(\equiv \frac{V}{V_G} \right) = 3 \quad (14)$$

$$\theta'_i \left(\equiv \frac{\theta_i}{\theta} \right) = \frac{1}{1 + \chi_0} = \frac{1}{4} \quad (i=1 \text{ to } 4). \quad (15)$$

We introduce here some known information [2] that the speed of the torso gravity centre against the absolute coordinate in a standard crab walk is one third of the return speed of the leg to the gravity centre, and that the distance advanced by the gravity centre during the return of each leg is the same for all the legs. Optimum condition A is realized in its basic equation (6) as functions of the circular radius r_G and foot-tip path radius r_i ($i=1$ to 4) only, so that it is determined regardless of the reachable range and the order of leg return.

6. SETTING THE ORDER OF LEG RETURN

In the case of creep gait, one of the legs returns under any condition. Therefore, the order of leg return in the case of circular gait of a quadruped walking machine cannot be more than six combinations in a circle permutation, i.e. ${}_4P_4/4$. The pattern is shown in Fig. 3. It has been known for a long time that four-legged animals have such six basic patterns of walk [6]. Frank and McGhee stated [7] that static stable walk in the x -direction was possible by selecting proper gaits in (1), (5) and (6) (Fig. 3), while it could not be realized in (2), (3) or (4). In particular, they called type (1) crawl gait, which they proved to be the most stable gait in x -directional locomotion. We investigated the order of leg return and found that the six combinations of return order shown in Fig. 3 were not merely a convenient theoretical classification but a

rational categorization covering all the return orders to be used in circular gait. Figure 3 (1) shows the crawl gait during a walk in the x -axis direction, (2) corresponds to crawl gait in the negative direction of the x -axis, (3) to the positive direction of the y -axis and (4) to the negative direction of the y -axis when they are classified from the same viewpoint as (1). That is, the four represent crawl gait in all the moving directions. Besides, (5) and (6) represent a sequential gait, which has the highest stability as well as efficiency of spin-turn when the turning centre is located close to the gravity centre. (5) Corresponds to counterclockwise walk and (6) to clockwise walk.

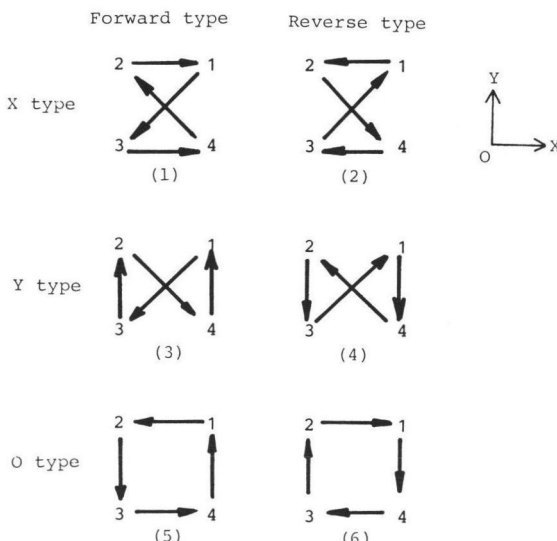


Figure 3. Classification of standard crawl gait. The arrow indicates the swing leg sequence.

On inducing the standard pattern in the circular gait around a random turn centre, we will determine initially the forward or reverse type as given in Fig. 3, and subsequently discuss all three types of leg return order—the X, Y and O types. The optimum pattern in each gait will be ultimately chosen from among the X, Y and O types satisfying optimum conditions A and B.

7. GAIT REALIZING OPTIMUM CONDITION B

The gait that realizes optimum condition B is given as the solution of a non-linear planning problem when the order of leg return is fixed:

Independent variable: ϕ_i , ($i = 1$ to 4), θ

Evaluation function: $\theta \rightarrow \max$

Restricting conditions: (a) static stability

(b) foot-tip reachable range.

Here, the initial landing point I_i of a foot-tip in the coordinates of the gravity centre is shown only by the argument θ_i of the polar coordinate, as the foot-tip circular radius r_i is already given.

The restricting condition (a) corresponds to prerequisite (3) for discussing walk

with zero-allowance of stability, in which the condition ‘the gravity centre is always located within the supporting triangle or on its periphery throughout a cycle’ is stated. This condition leads to a non-linear equation and an inequality restriction in X or Y type order of leg return, and a non-linear inequality restriction in the O type.

In this way, the nature of the problems is different for the X, Y types and the O type. The same discussion is possible for the X and Y types because the x/y-axes of the Y type are just the opposite of those of the X type. Therefore, hereafter, only the X and O types will be studied for the orders of leg return.

7.1. Maximization of the circular angle in the X type

First, the restricting conditions will be established in equations and second, the optimum solution will be induced.

7.1.1. Equational restriction for static stability. In the X type leg return sequence shown in Fig. 4, when one of the forelegs U completes its return, the hindleg C at the diagonal position begins the returning motion. Therefore, the supporting triangle of the gravity centre keeps shifting, for instance, from ΔABC to ΔABU with the side \overline{AB} in contact, every time a foreleg lands during the locomotion. This is the moment when a vehicle has the lowest stability in the X type walk. Accordingly, the moment will be called the ‘switching point’, the side connecting leg A to leg B will be called the ‘switching side’ and legs A and B will be called ‘switching legs’. Of the switching legs, the foreleg is set A and the hindleg B. If the gravity centre is not on the switching side at the switching point, static stability is not satisfied either before or behind the switching point. In other words, the primary condition for static stability is that the gravity centre should be on the switching side at any switching point.

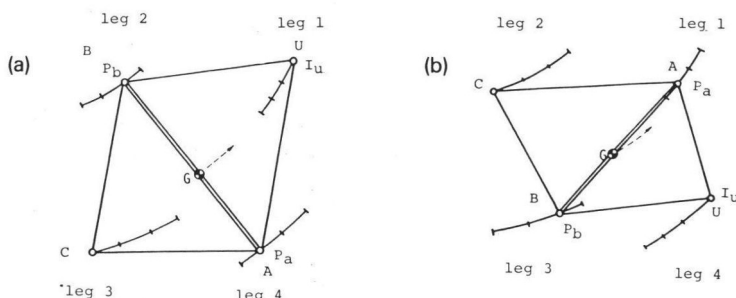


Figure 4. Static stability conditions of the X-type standard circular gait.

To describe the conditions for static stable walk, it is more convenient to use the foot-tip positions P_a and P_b of the switching legs A and B at two points of time when the gravity centre is on the switching side instead of using the initial landing point I_i of each leg. It is possible to obtain I_i of leg i based on P_i as the leg return sequence is fixed because, in the case of leg A, after obtaining argument ϕ_{P_a} indicating the position of P_a , the argument ϕ_{I_a} of I_a is given as $\phi_{I_a} = \phi_{P_a} + \theta_b + \theta_u$ using the turning angles θ_b and θ_u of the gravity centre when legs B and U are returning.

In order to describe the positions of the gravity centre and foot-tips on the basis of $P_i(r_i, \theta_i)$ and $G(r_G, \theta_G)$ shown by the polar coordinate with turn centre Q as the origin, the conditional equation for the gravity centre G being on the switching

side is effected in two cases when the switching legs A and B in a cycle are the first and third legs and the second and fourth legs, respectively, and they are respectively expressed by non-linear equations. The expression regarded as the simplest is the following one, which indicates the area S of the triangle formed by the switching legs and the gravity centre is 0:

$$S(\phi_{Pa}, \phi_{Pb}, \phi_G) = r_a r_b \sin(\phi_{Pb} - \phi_{Pa}) + r_b r_G \sin(\phi_G - \phi_{Pb}) + r_G r_a \sin(\phi_{Pa} - \phi_G) = 0 \quad (16)$$

where $b=3$ when $a=1$ and $b=2$ when $a=2$.

7.1.2. Inequality restriction for static stability. Another condition for static stability, in addition to those stated above, is that the gravity centre continues to stay within the supporting triangle ABU while leg C is returning, even in the case of Fig. 4(b) in which the turn centre Q is located close to the gravity centre G and the moving path has a large curvature. Such a restriction is necessary in the circular movement in which the turn centre Q is located at the position to effect $r_G < \min(r_a, r_b)$. Specifically speaking, as shown by Fig. 5, it is a condition that the centre angle 2σ of the arc GX of the gravity centre path cut by the switching side AB is larger than the turning angle θ_c during the return movement of leg C. It can be written as

$$\begin{aligned} \theta_c &= \theta \cdot \theta'_c \leq 2\sigma \\ \therefore \theta &\leq \frac{2}{\theta'_c} \sigma = \frac{2}{r'_i} \times \tan^{-1} \frac{r_G - r_a \cos(\phi_{Pa} - \phi_G)}{r_a \sin(\phi_{Pa} - \phi_G)} \end{aligned} \quad (17)$$

where $c=2$ when $a=1$ and $c=3$ when $a=4$.

Here, θ'_c is a known figure denoting the ratio of turning angle during the return cycle of leg C which is induced by equations (11) and (12) for optimizing the speeds which satisfy optimum condition A. Equation (17), which is a non-linear inequality effected between θ and either of the arguments ϕ_{P1} and ϕ_{P4} , provides the additional condition for maintaining static stability.

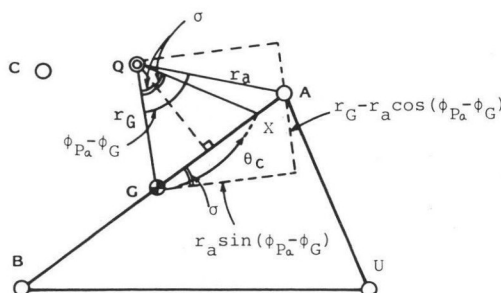


Figure 5. Additional condition for static stability.

7.1.3. Inequality restriction by reachable range. This is obtained, for instance in the case of Fig. 6, by the relations of the argument ϕ_{I_1} ($=\phi_{P1} + \theta_3 + \theta_4$) of point I_1 of leg 1 to be smaller than the argument ϕ_{F_1} of point F_1 and the return initiating point

$(\phi_{p_1} - \theta_2)$ to be larger than the argument ϕ_{R_i} of point R_i . They are expressed by simple inequalities as follows:

$$\begin{cases} \phi_{p_i} + k_{F_i} \cdot \theta \leq \phi_{F_i} \\ \phi_{p_i} - k_{R_i} \cdot \theta \geq \phi_{R_i} \end{cases} \quad (i=1 \text{ to } 4) \quad (18)$$

where k_{F_i} and k_{R_i} are given in Table 1.

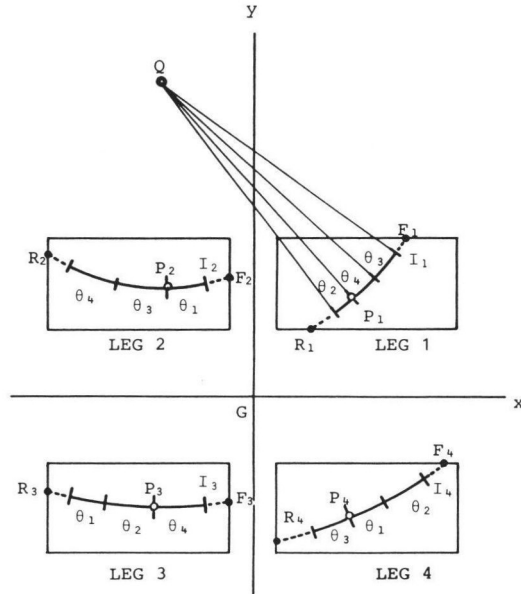


Figure 6. Relation between X type standard circular gait and reachable area.

7.1.4. *Induction of optimum solution.* We have thus obtained the relation to be effected between θ and ϕ_{p_i} ($i=1$ to 4). Next the solution will be presented.

Table 1.
The coefficient k of equation (18)

Leg number i	k_{F_i}	k_{R_i}
1	$\theta'_{3'} + \theta'_{4'}$	$\theta'_{2'}$
2	$\theta'_{1'}$	$\theta'_{3'} + \theta'_{4'}$
3	$\theta'_{4'}$	$\theta'_{1'} + \theta'_{2'}$
4	$\theta'_{1'} + \theta'_{2'}$	$\theta'_{3'}$

The problem has some restricting conditions characterized as follows: Equation (16) contains two ϕ_{p_i} , while inequalities (17) and (18) contain either of ϕ_{p_i} and θ only. θ has a monotonic boundary with ϕ_{p_i} . Therefore, the problem can be broken down into two inequality spaces: $\theta - \phi_{p_1} - \phi_{p_3}$ and $\theta - \phi_{p_2} - \phi_{p_4}$. As equation (16) is effected,

the problem can be reduced to simple equations which optimize θ for the ϕ_{p_i} . The image is shown in Fig. 7.

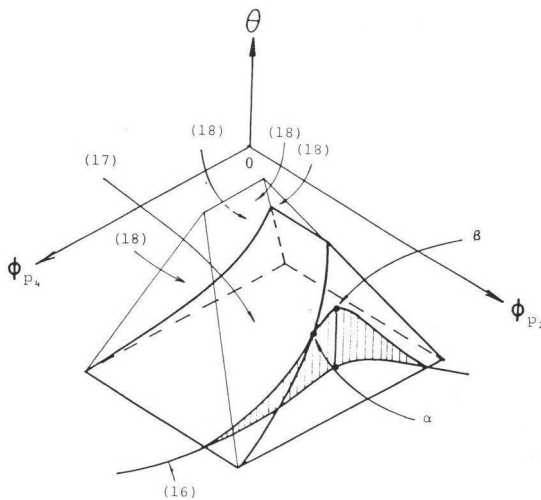


Figure 7. Geometrical image of the optimization B problem for X type standard circular gait.

Therefore, the optimum solutions are limited to:

- (1) intersection (point α in Fig. 7) of the ridge of the boundary between equations (17) and (18) with the curved surface of equation (16); and
- (2) intersection (point β in Fig. 7) of the straight line passing through the maximum or minimum point of equation (16), $\phi_{p_i} = F(\phi_{p_a})$, and being parallel to the θ -axis, with the boundary between equations (17) and (18).

Therefore, it is possible to obtain the solution without resorting to convergence calculation. The solution θ of the problem is in general the smaller one of the maximum values obtained in each space of $\theta - \phi_{p_1} - \phi_{p_3}$ and $\theta - \phi_{p_2} - \phi_{p_4}$.

A concrete solution of this problem will be presented in Section 8.1.

7.2. Maximization of the turning angle in the O type

The most conspicuous difference from the case of the X type is that the stability of the O type is much better. As the returning leg always shifts to the adjacent leg in the O type, the movement of the supporting triangle always has an overlap. As the O type is more stable than the X type, the calculation for optimization is not restricted by equations but by inequalities only.

7.2.1. Inequality restriction for static stability. The conditions of static stability when a random leg U is returning will be discussed in this section. In this discussion, the coordinate will be the absolute polar coordinate with the turn centre Q as the origin. This coordinate system will be set so as to make the shifting direction of the gravity centre at initiation of the return of leg U the x -axis of the absolute polar coordinate. Legs A, C and B are defined to be the leg which returns behind leg U in that order. Their positions at the switching points will be expressed, respectively, as $A(r_a$ and ϕ_{p_a}), $C(r_c$ and ϕ_{p_c}) and $B(r_b$ and ϕ_{p_b}). The switching point in the O type is the

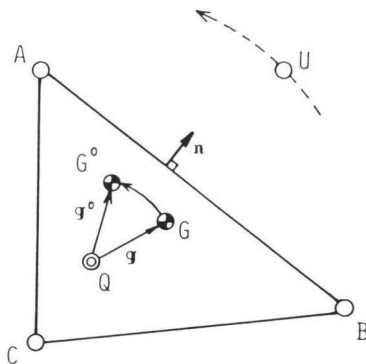


Figure 8. Static stability condition of O-type standard circular gait.

moment when leg U initiates return motion. The positions of returning leg U at the switching point and on completing the return will be expressed by $G(r_G)$ and $G^*(r_G, \phi_G) [=G(X_G, Y_G)]$ and $G^*(r_G, \phi_{G^*})$, respectively.

Figure 8 shows the concrete case of the leg geometry defined as above. Here, r_a , r_b and r_c were obtained in preliminary calculations. The other variables are given by

$$\phi_G = \tan^{-1} (Y_G/X_G) \quad (19)$$

$$\phi_{G^*} = \phi_G + \theta'_u \cdot \theta \quad (20)$$

$$\phi_{P_a} = \phi_{I_a} - (\theta'_B + \theta'_C) \cdot \theta \quad (21)$$

$$\phi_{P_b} = \phi_{I_b}. \quad (22)$$

It is impossible for the gravity centre to move from sides AC and BC in the usual foot reachable range (see Fig. 8). Accordingly, the conditions for stability will be induced with respect to side AB. Using the function S of equation (16), we can express the relation as follows:

In all $G^* \in [G, G^*]$

$$S(\phi_{P_a}, \phi_{P_b}, \phi_{G^*}) \leq 0 \quad (23)$$

where

$$\phi_{G^*} = \begin{cases} \phi_G & \phi \in [\phi_G, \phi_{G^*}] \text{ and } \cos(\phi_G - \phi_n) \geq \cos(\phi_{G^*} - \phi_n) \\ \phi_n & \phi_n \in [\phi_G, \phi_{G^*}] \\ \phi_{G^*} & \phi_n \notin [\phi_G, \phi_{G^*}] \text{ and } \cos(\phi_G - \phi_n) < \cos(\phi_{G^*} - \phi_n). \end{cases}$$

ϕ_n is the directional angle of the normal vector n of AB.

Equation (23) was obtained based on the condition that $\triangle ABG^*$, formed by the point G^* on the ray of the gravity centre GG^* with A and B, has a negative area, i.e. ABG^* turns clockwise. The conditions of static stability during the returning motion of leg U are given as the relations among $\theta - \phi_{11} - \phi_{13}$, $\theta - \phi_{12} - \phi_{14}$ from equation (23). Consequently, the conditions of static stability throughout a cycle should assure the relations for all legs U equal to 1 to 4.

7.2.2. Inequality restriction based on reachable range. The reachable range condition in the O type is expressed by a linear inequality restriction similar to that

of the X type as follows:

$$\begin{cases} \phi_{li} & \leq \phi_{Fi} \\ \phi_{li} - (1 - \theta'_i) \cdot \theta & \geq \phi_{Ri} \end{cases} \quad (i=1 \text{ to } 4). \quad (24)$$

7.2.3. Induction of the optimum solution. Thus the relation to effect between θ and ϕ_{li} has been established. Next the method of solution will be discussed.

The O-type problem cannot be solved by any specific method, as in the X type problem. Therefore, the problem was solved by the convergence calculation based on a multiplying method [8] which was one of the non-linear programs. This method was used to obtain the local optimum solution. As it was not assured that the solution was the only one in this problem, the starting point of the convergence calculation should be questioned. We began the convergence based on a pseudo-optimum solution excluding the non-linear restriction within the range employed in this study. The solution was regarded as sufficiently reliable. This was also proved by the result of a comprehensive simulation using a computer.

8. INDUCTION OF STANDARD CIRCULAR GAIT AND EXPERIMENT BASED ON MACHINE MODELS

8.1. Induction of standard circular gait

The reachable range of a walking vehicle was set as shown in Fig. 2, and the standard circular gait was induced in the case where the turn centre Q was at a random point. One of the results is shown in Fig. 9(a).

Figure 9(a) is an example of inducing the foot-tip path of the standard circular gait in which the return leg sequence is the X type, the circular radius is 1 m, and the circular crab walk angle a_Q is 15° . For the purpose of comparison, Fig. 9(b) is shown as an example of gait which satisfies optimum condition B only under the condition of $\theta'_i = \theta_i / \theta = 1/4$ ($i=1$ to 4). The condition of uniform angular speed is easily derived from the analogy of standard crab walk.

Comparison of (a) and (b) indicates that the standard circular gait (a) proposed in this paper has improved the peripheral speed by nearly 50% and the turning angle in a walk of one cycle walk by 24% over the conventional approach of (b). The turning angle increases as a result of adding optimum condition A, because the closer the legs are located to the centre Q, the larger is the arc angle of foot-tip path, so that the reachable range is used more efficiently.

This effect was investigated at a circular crab walk angle ($a_Q = 15^\circ$) by changing the circular radius. The result is shown in Fig. 10. It can be seen that the closer the turning centre gets to the gravity centre from the crab walk gait ($1/r_G = 0$) and the larger is the curvature ($1/r_G$ —large), the more the reciprocal argument among θ_i enlarges to give the optimum gait [Fig. 10(b)] and consequently both the speed and the circular locomotion distance increase in comparison with the case (dashed line) where θ_i is simply set uniform [Figs. 10(a) and 10(c)].

Next, comprehensive calculations are done on circular gaits each having the turning centre Q at locations within quadrant II on the coordinates of the gravity centre, and turning angles of the gravity centre, θ_{rad} , of the gait satisfying optimum conditions A and B are obtained for each leg-return sequence of the X, Y and O

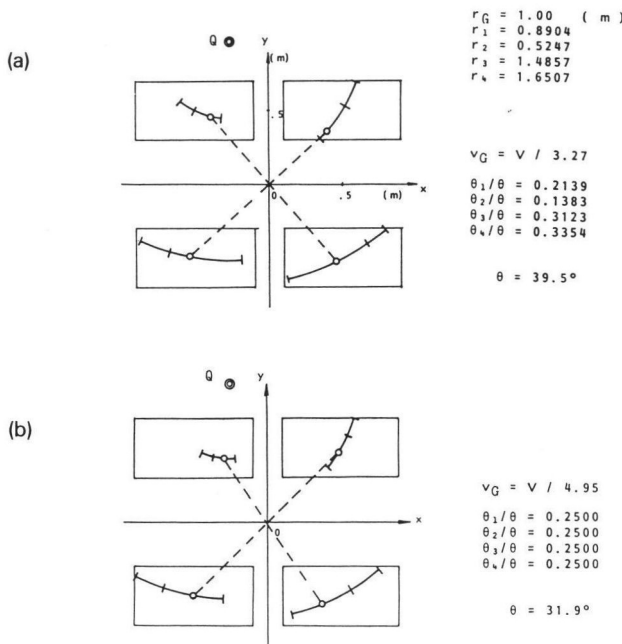


Figure 9. One of the gait examples derived by the theory. (a) Gait with optimization A and B; (b) gait with optimization B.

types. The values are plotted in the form of contour lines as shown in Figs 11(a), 11(b) and 11(c). Based on these conditions, the sequence which takes the largest turning angle θ , among the three types of leg-return sequence (X, Y and O types), when the turning centre Q is at a random position is selected. The value of θ at this time and the leg-return sequence providing the status are shown in a "status chart" [Fig. 11(d)]. As the walking vehicle is symmetric on the right/left and front/back, the information is effective when point Q is anywhere on the plane. The regions labelled X or O type in Fig. 11(d) have common restrictive conditions so that either gait gives the same θ . Concrete examples of the standard circular gaits of the X, Y and O types are shown in Figs 12(a), 12(b) and 12(c).

8.2. Experiment by machine model

The standard circular gait thus induced was actually realized in the TITAN III, a quadruped walking vehicle, shown in Fig. 13.

TITAN III weighs 80 kg and has four legs, each 1.2 m long. It walks with the aid of 12 software servo-actuators controlled by a PC-9801 computer. The control system is an adapted C compiler (CI-C86). At present, the sampling interval to produce the target value is 50–150 ms.

Figure 14 shows an example of the TITAN III moving experiment in which the body turn in the O type standard circular gait. The trajectories of two lamps on top of the body indicate the state of the turn. The turning time in one cycle was 14 s and the angle was 35°. The standard circular gait calculated off-line was given as a table for execution. The same walking experiments were also conducted for the X and Y types.

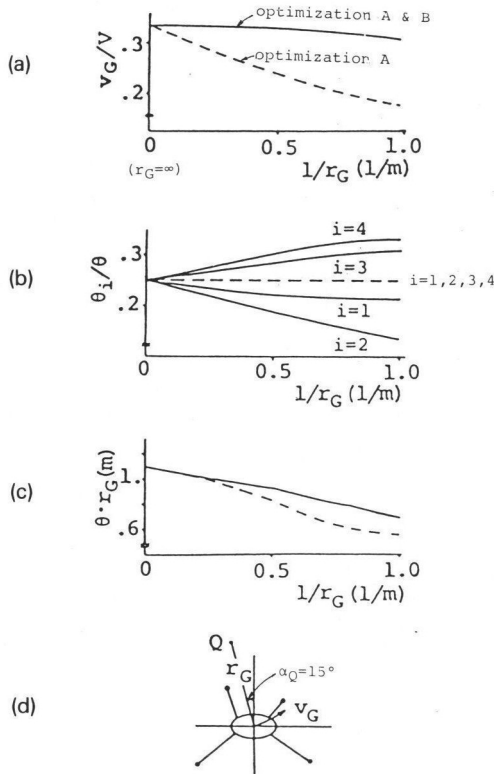


Figure 10. The effect of optimization A and B. (a) Circular radius vs. circular velocity; (b) circular radius vs. swing angle of each leg; (c) circular radius vs. body's rotation distance in unit cycle; (d) relation between turning centre Q and body of the above example [(a), (b), (c)].

The mechanism and controls of TITAN III have been reported in details elsewhere [3]. We believe that the walking experiment proves the effectiveness of the standard circular gait, induced in the present study, for controlling practical walking machines.

In order to realize real-time generation of the standard circular gait, the operations stated in Section 3 should be performed successively. In this case, it would be more convenient if the leg-return sequence of (3) in Section 3 was obtained by preliminarily plotting a 'status chart' [Fig. 11(d)] based on the location of the turning centre Q, and then executing a calculation only for the selected leg-return sequence.

9. CONCLUSIONS

The present study has discussed the standard patterns of a circular gait of a quadruped walking vehicle from two viewpoints of optimization and has presented the specific inducing method. The effectiveness of the technique is proven by the calculation simulation and the experiment using a quadruped walking vehicle model. Furthermore, we intend to coordinate the results of this study with a lower control system, such as up/down motion of legs, and an upper control system, such as ground-adapting walk, so as to induce a circular-gait-determining algorithm having a more general and practical application. The standard circular gait and inducing

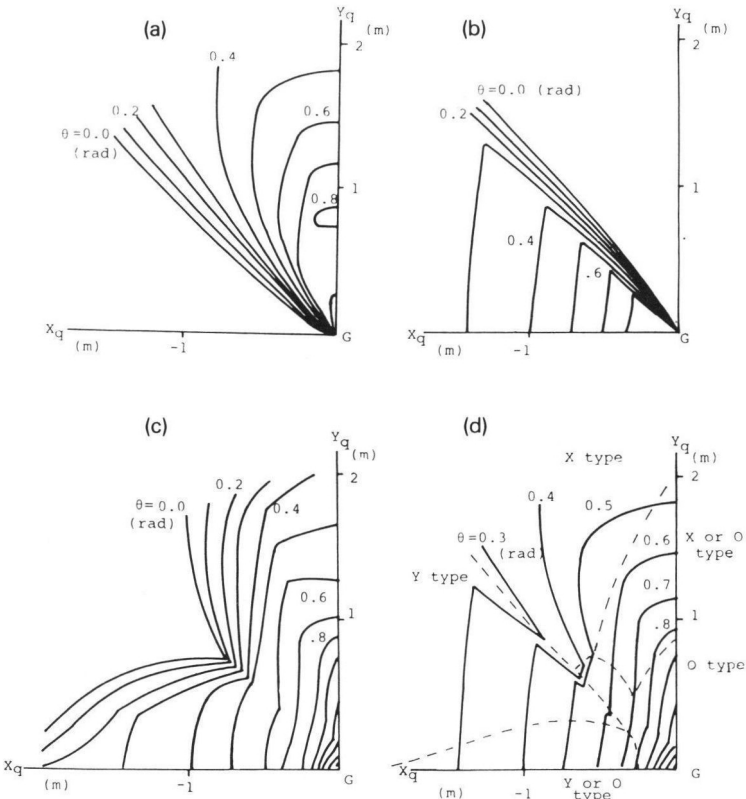


Figure 11. Selection of the circular gait types and maximum turning angle θ for any location of turning axis Q. (a) Maximum turning angle of X type circular gait; (b) maximum turning angle of Y type circular gait; (c) maximum turning angle of O type circular gait; (d) optimum selection of the swing-leg sequence.

method discussed in this paper are based only on a vehicle having a rectangular reachable range as shown in Fig. 1; nevertheless, it should be mentioned that the approach can be applied to any four-legged robot having any type of reachable range.

REFERENCES

1. S. Hirose, H. Iwasaki and Y. Umetani, "Fundamental studies on determining intelligent gait of quadruped walking vehicle," *SICE J.*, vol. 18, no. 2, pp. 193–200, 1982.
2. S. Hirose, M. Nose, H. Kikuchi and Y. Umetani, "Adaptive gait control of a quadruped walking vehicle," *Proc. 1st ISRR*, Bretonwoods, 1983.
3. S. Hirose, T. Masui, H. Kikuchi, Y. Fukuda and Y. Umetani, "Structure and basic properties of quadruped walking vehicle TITAN III," *Monograph of 2nd Intelligent Mobile Robots Symp.*, 1984, pp. 13–19.
4. R. B. McGhee and A. A. Frank, "On the stability properties of quadruped creeping gait," *Math. Biosci.*, vol. 3, no. 3, pp. 331–351, 1968.
5. R. Tomović, "A general theoretical model of creeping displacement," *Cybernetica*, vol. 4, no. 2, 1961.
6. P. P. Gambaryan, *How Mammals Run*, New York: Wiley, 1974.
7. A. A. Frank and R. B. McGhee, "Some considerations relating to the design of autopilots for legged vehicles," *J. Terramechanics*, vol. 6, no. 1, pp. 23–35, 1969.
8. S. Konno and T. Yamashita, *Non-linear Planning Method*, Nikkagiren, 1978.

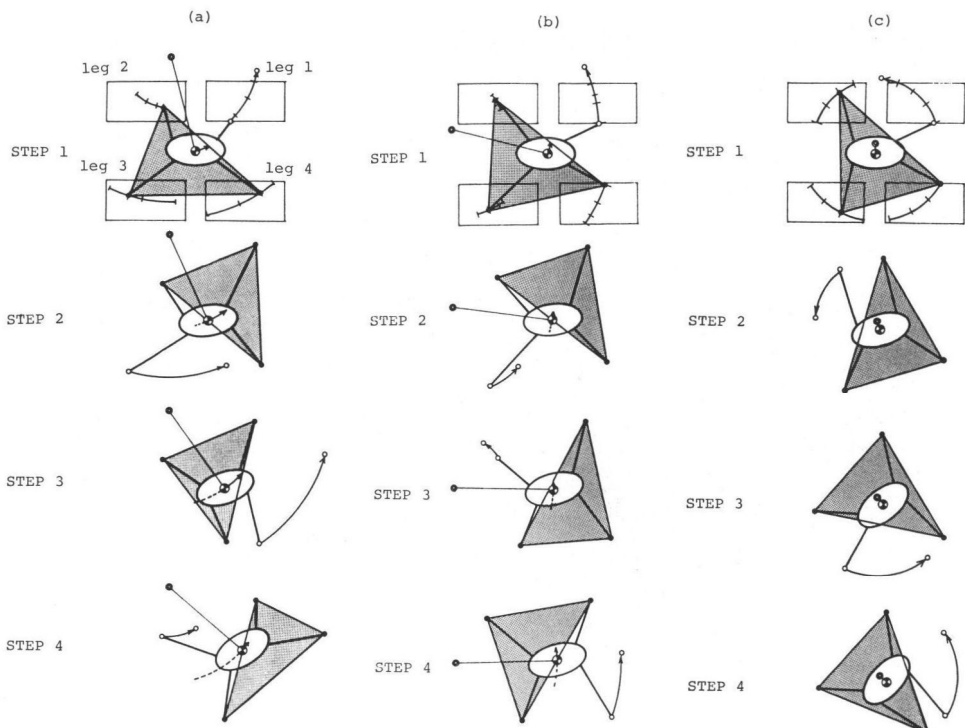


Figure 12. Gait examples of standard circular gait. (a) X type, turning radius 1 m, circular crab angle 15°; (b) Y type, turning radius 1 m, circular crab angle 5°; (c) O type, turning radius 0.1 m, circular crab angle 0°.

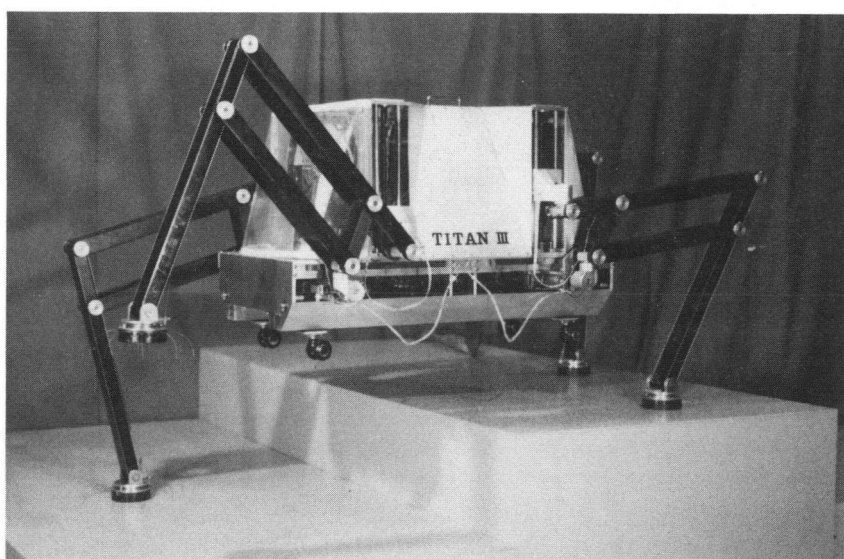


Figure 13. The constructed quadruped walking vehicle model, TITAN III.

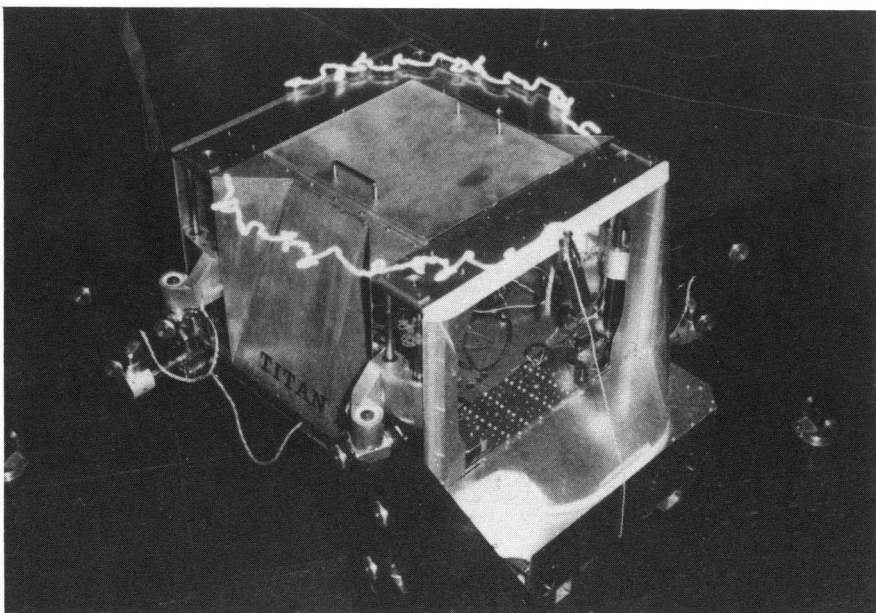


Figure 14. Circular gait on the spot. The body motion is shown by the trajectories of the lamps attached on the top of the body.

APPENDIX

Under the assumption

$$v_g \leq \frac{V}{\chi_i} \quad (A1)$$

$$\chi_i = r'_i \left(\frac{1}{\theta'_i} - 1 \right) \quad (A2)$$

$$\sum_{i=1}^4 \theta'_i = 1 \quad (A3)$$

$$(i=1 \sim 4)$$

$$V, r'_i: \text{constant}$$

The proof that the maximum solution v_g^* of $v_g(\chi_1, \chi_2, \chi_3, \chi_4)$ are

$$\chi_1 = \chi_2 = \chi_3 = \chi_4 = \chi_0 \quad (A4)$$

is done by using paralogism. Assume that a maximum solution $v_g^*(\chi_1^\Delta, \chi_2^\Delta, \chi_3^\Delta, \chi_4^\Delta)$ other than (A4) exist. In this case

$$v_g^\Delta \leq \frac{V}{\chi_i^\Delta} \quad (A1')$$

$$\chi_i^\Delta = r'_i \left(\frac{1}{\theta_i^\Delta} - 1 \right) \quad (A2')$$

$$\sum_{i=1}^4 \theta_i^\Delta = 1 \quad (A3')$$

$(i=1 \sim 4)$

and

$$v_G^\Delta > v_G^* \quad (A4')$$

At this time as to j that satisfy

$$\chi_j^\Delta = \max_{i=1 \sim 4} \chi_i^\Delta$$

produces

$$v_G^\Delta \leq \frac{V}{\chi_j^\Delta} \quad (A1')$$

from (A1'), (A4), (A4')

$$\frac{V}{\chi_j^\Delta} \geq v_G^\Delta > v_G^* = \frac{V}{\chi_0} = \frac{V}{\chi_j} \\ \therefore \chi_j^\Delta < \chi_j = \chi_0 \quad (A5)$$

substitutes (A2), (A2)

$$r'_j \left(\frac{1}{\theta_j^\Delta} - 1 \right) < r'_j \left(\frac{1}{\theta'_j} - 1 \right) \\ \therefore \theta_j^\Delta > \theta'_j$$

On the other hand from (A3), (A3') ($\theta_k^\Delta < \theta'_k$) holds true at $k=j$. Therefore

$$r'_k \left(\frac{1}{\theta_k^\Delta} - 1 \right) > r'_k \left(\frac{1}{\theta'_k} - 1 \right) \\ \therefore \chi_k^\Delta > \chi_0 = \chi_j \quad (A6)$$

As a result of (A5) and (A6)

$$\chi_k^\Delta > \chi_0 > \chi_j^\Delta.$$

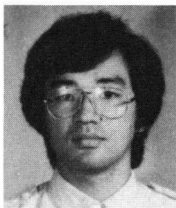
This result contradicts

$$\chi_j^\Delta = \max_{j=1 \sim 4} \chi_j^\Delta.$$

The value (A4) is thus proved to be an maximum solution.

ABOUT THE AUTHORS

Shigeo Hirose was born in Tokyo, Japan in 1947. He received his B.E. degree in Mechanical Engineering from Yokohama National University in 1971, and M.E. and Dr.E. degrees in Control Engineering from Tokyo Institute of Technology in 1973 and 1976, respectively. From 1976 to 1979 he was a Research Associate and he is at present the Associate Professor of the Department of Physical Engineering at the Tokyo Institute of Technology. His research interests are in the design of mechanisms, actuators, sensors and control systems of Robots.



Hidekazu Kikuchi was born in 1959. He received his B.E. and M.E. degrees in Physical Engineering from Tokyo Institute of Technology in 1982 and 1984, respectively. He is at present working at Asahi Chemical Industry Co. Ltd., Electronics Research Laboratory and is studying semiconductors.



Yoji Umetani was born in Osaka, Japan in 1932. He received his B.E. degree in Mechanical Engineering from Kyoto University in 1956, and Dr.E. degree from Tokyo Institute of Technology in 1968. From 1959 he was the Lecturer of the University of Tokyo. From 1970 he was the Associate Professor of the Tokyo Institute of Technology. From 1975 till now he is the Professor of Department of Physical Engineering at the Tokyo Institute of Technology. His research interests are in the study of process control, biomechanics, and robotics.